



# Uncertainty quantification for nonlinear seismic analysis of cabinet facility in nuclear power plants

Thanh-Tuan Tran<sup>a,b</sup>, Dookie Kim<sup>a,\*</sup>

<sup>a</sup> Department of Civil Engineering, Kunsan National University, Gunsan si, Republic of Korea

<sup>b</sup> Faculty of Technology and Technique, Quy Nhon University, Binh Dinh Province, Viet Nam



## ARTICLE INFO

### Keywords:

Cabinet facility  
Uncertainty quantification  
Random field  
Seismic analysis  
Analytical model  
Shaking table test

## ABSTRACT

Effects of spatial variability of structural properties on seismic responses of cabinet facility in the nuclear power plant are investigated. For the nonlinear behaviour of the cabinet, the effects of the softening and axial force are investigated through the analytical model. The accuracy of the model is verified against the experimental tests. To account for the randomness of material and geometrical properties, input variables are treated as random variables and produced with the random field theory. An efficient method using the combination of a covariance matrix decomposition (i.e. Cholesky, Eigen, and modified Cholesky decompositions) and a midpoint discretization method is proposed and it is implemented for the stochastic response analyses of structures. The effectiveness of the method is evaluated with the dispersion and uncertainty of output responses. It is found that the heterogeneity of material properties has a strong influence on the seismic vulnerability assessment of cabinet facility, and the performance of modified Cholesky decomposition is better than other methods in generating random fields.

## 1. Introduction

The non-structural components in a structure like electric cabinets play an important role in nuclear power plants (NPPs). The safety of this equipment must be evaluated to demonstrate its abilities under earthquake excitations. The seismic performance of these non-structures has been investigated in a few studies (Cho et al., 2011; Hur, 2012). The researchers have focused on the risk assessment of the dynamic behaviour of cabinet structures by modelling the finite element models (Lim, 2016; Tran et al., 2019) or on performing experimental tests (Bandyopadhyay et al., 1987; Cho et al., 2011; Kim et al., 2012; Koo et al., 2010; Nguyen and Kim, 2014). Hur (2012) developed a simplified model for cabinets that includes the frame and shell elements for structural elements. In this model, the connections between framing members and panels have been modelled using the nonlinear springs. Gupta et al. (1999) proposed a method using the Ritz vector approach to accurately evaluate the in-cabinet response spectra for seismic qualification of cabinet structures. The method was then modified by Gupta and Yang (2002) to overcome limitations that were encountered during applications to actual cabinets. Recently, the safety assessments of NPP and its equipment have been investigated by fragility curves using the lognormal approaches (i.e. maximum likelihood estimation, linear regression) or artificial neural networks (ANN) (Nguyen et al., 2019; Thai and Kim, 2015; Tran et al., 2018a,b, 2019; Wang et al., 2018).

The structural behaviours associated with the uncertain input variables can be predicted using the stochastic approach. This approach has been presented for various structures in many works (Eem and Kim, 2019; Jenkel et al., 2015; Kala, 2011; Kotelko et al., 2017; Sahu et al., 2019; Yue and Ang, 2017). Kotelko et al. (2017) investigated the effects of input variables (i.e. material and geometrical parameters) of box-section girders due to pure bending using the Monte Carlo simulations. Kala (2011) and Jenkel et al. (2015) studied the sensitivity and reliability analysis of steel plane frames and timber structures considering the variability in material properties. Likewise, Yue and Ang (2017) carried out the stochastic response and reliability of the tunnel-soil system using the random field theory. In the field of geotechnical engineering, various researchers studied the randomizations of geotechnical properties (Griffiths et al., 2009; Tran et al., 2018a,b; Xu, 2011). Griffiths et al. (2009) reported the effects of spatial uncertainty on slope reliability through the random finite element method, combining from a finite element model and random field model (Vanmarcke, 1982, 2010). However, in the case of cabinet facility, the consideration of system parameters is still limited. Thus, it is necessary to develop a technique to accurately predict the nonlinear behaviour of cabinet structures due to earthquake loadings, particularly when the material and geometrical parameters are varied. In the present work, the spatial variability of these input variables is captured with the random field theory.

\* Corresponding author at: Department of Civil Engineering, Kunsan National University, 558 Daehak-ro, Gunsan-si 573-701, Jeollabuk-do, Republic of Korea.  
E-mail addresses: [tranhanhtuan@kunsan.ac.kr](mailto:tranhanhtuan@kunsan.ac.kr) (T.-T. Tran), [kim2kie@kunsan.ac.kr](mailto:kim2kie@kunsan.ac.kr) (D. Kim).

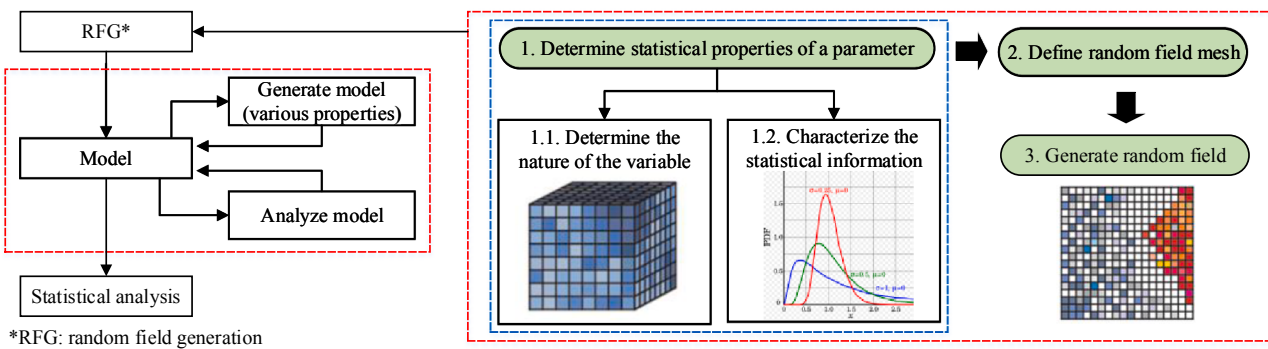


Fig. 1. The schematic diagram for the stochastic analysis framework.

In addition, the configuration, mass, and stiffness of the cabinet facility can vary due to the uncertainties of the structure (i.e. geometrical and material parameters). Therefore, the finite element model is complex and difficult to apply for practical use in probabilistic simulation. In this study, a beam stick model is developed in practice to represent the structural behaviour subjected to earthquake loadings. The effects of axial force and Duffing's type of the restoring force are taken into account while investigating the nonlinear seismic behaviour of cabinets. Experimental tests have also been performed to verify the accuracy and efficiency of the proposed model.

The above discussions lead to the question of how to model and quantify the randomness of structural properties of a cabinet facility in NPPs. This research aims to address this challenge using the probabilistic nonlinear analysis. A schematic diagram of the stochastic analysis is illustrated in Fig. 1. Firstly, a random field generator is used to generate uncertainties of input variables. Then, time history analysis for the structure is conducted. The procedure is repeated for each combination of input variables defined in the structural model. Finally, the statistical characteristics of the response (i.e. the mean, the standard deviation, and the covariance of variable) are obtained.

## 2. Random fields

According to Vanmarcke (2010), a random field can be depicted as a continuous function related to the random variable in time and space. The random field can be defined in one-dimension  $H(x, t)$  where  $x$  is a spatial variable, or in multiple-dimensions  $H(\mathbf{x}, t)$  where  $\mathbf{x}$  is a vector that contains spatial variables (Van der Have, 2015). Several techniques have been presented to generate a random field (Griffiths et al., 2009; Yue and Ang, 2017). These methods are classified into two categories as shown in Fig. 2. The first class is a combination of spatially correlated variables and a discretization method. The second class is based on the series expansion methods that the random field is represented as a sum of functions multiplied by random variables.

In this study, the input variables of structural properties are examined using the class I, where the random field generator based on the Covariance Matrix Decomposition (CMD) along with a Midpoint Discretization Method (MPM) is applied. This methodology can consider the uncertainties of input parameters. Firstly, the correlation matrix is assembled with a correlation function (Section 2.1). Then, the decomposition correlation matrix is decomposed by various methods (Section 2.2). The procedure is summarized as follows:

- Given a sequence of points in the random field,  $\mathbf{X} = \{X_1, X_2, \dots, X_n\}^T$ , then the values of  $\mathbf{X}$  can be expressed in the form of

$$\mathbf{X} = \boldsymbol{\mu} + \mathbf{z}_c(\mathbf{x}) \quad (1)$$

where  $\boldsymbol{\mu}$  is the mean at each point in the field, and  $\mathbf{z}_c(\mathbf{x})$  is the vector containing spatially correlated random variables.

- The random variables are generated using the CMD and determined using the following equation

$$\mathbf{z}_c(\mathbf{x}) = \mathbf{LG} \quad (2)$$

where  $\mathbf{G}$  is the vector of independent zero mean, unit variance, normally distributed random variables;  $\mathbf{L}$  is a decomposed correlation matrix and can be taken by different methods such as Cholesky decomposition (CHOL), Eigen decomposition (EIG), and modified Cholesky (MCHOL) decomposition.

### 2.1. Correlation matrix

In statistical analysis, covariance is a measure of the variability of two variables, and a covariance function depicts the spatial covariance of a random variable process. For a random field, the covariance function,  $C_{X_{ij}}$ , gives the covariance of the values at the two points ( $i$  and  $j$ )

$$C_{X_{ij}} = \text{Cov}(i, j) \quad (3)$$

The correlation function is related to covariance function and is given by

$$\rho_{ij} = \frac{C_{X_{ij}}}{\sigma_i \sigma_j} \quad (4)$$

where  $\sigma_i$  and  $\sigma_j$  are standard deviations of two points ( $i$  and  $j$ ). Generally, the correlation function can be expressed using the following models

- Exponential correlation

$$\rho_{ij} = \rho(\xi_{ij}) = \exp\left(-\frac{\xi_{ij}}{l_{corr}}\right) \quad (5)$$

- Square exponential correlation

$$\rho_{ij} = \rho(\xi_{ij}) = \exp\left[\left(-\frac{\xi_{ij}}{l_{corr}}\right)^2\right] \quad (6)$$

- Sinusoidal correlation

$$\rho_{ij} = \rho(\xi_{ij}) = \frac{\sin\left(-2.2 \frac{\xi_{ij}}{l_{corr}}\right)}{-2.2 \frac{\xi_{ij}}{l_{corr}}} \quad (7)$$

where  $\xi_{ij}$  is the lag distance between point  $i$  and  $j$ ;  $l_{corr}$  is the correlation length, which represents a measure of the variable fluctuations in the random field.

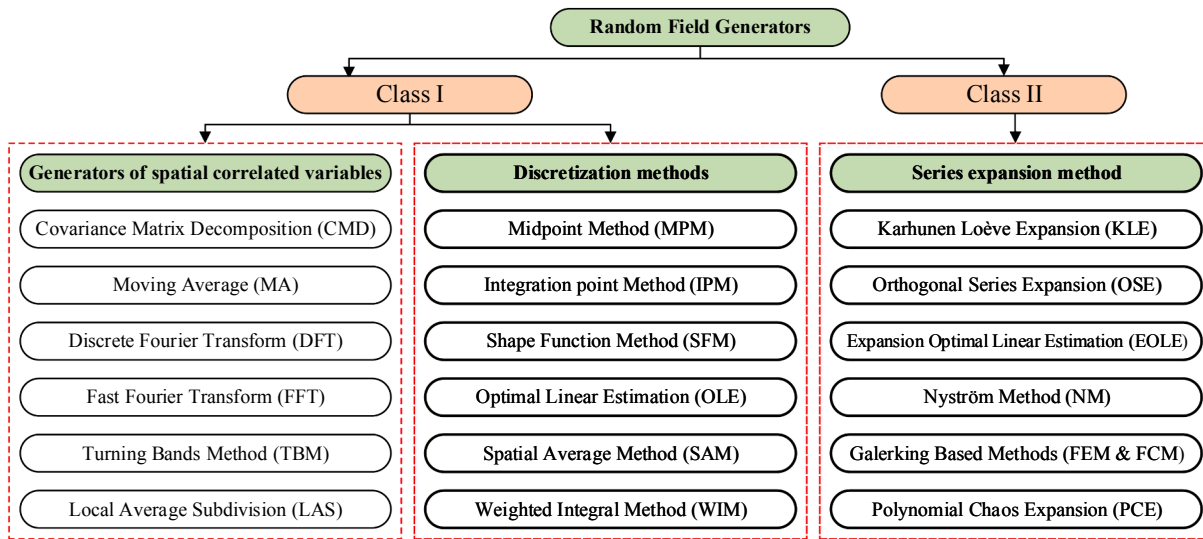


Fig. 2. Classification of random field generators (Van der Have, 2015).

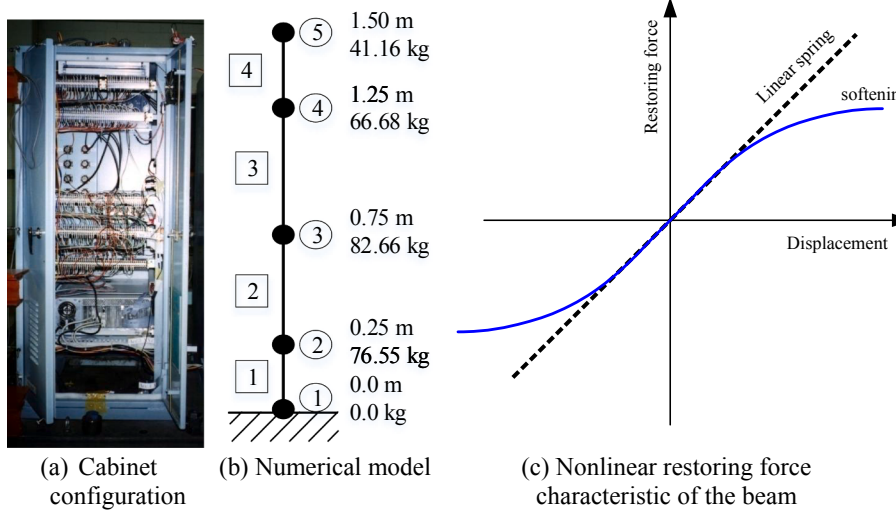


Fig. 3. Schematic view of the cabinet (Cho et al., 2011).

## 2.2. Decomposition methods

The decomposition of the correlation matrix,  $\rho'$ , can be derived using the following methods.

- Cholesky decomposition (CHOL)

$$\rho' = \mathbf{L}\mathbf{L}^T \quad (8)$$

where  $\rho'$  is the symmetric positive matrix, and  $\mathbf{L}$  is the lower triangular matrix. The diagonal terms are obtained by taking the square root of the corresponding diagonal term in the correlation matrix, which is subtracted by squared values of the corresponding rows of the decomposed matrix

$$L_{kk} = \sqrt{R_{kk} - \sum_{j=1}^{k-1} L_{kj}^2} \quad (9)$$

where  $k$  is equal to the row number of the computed diagonal element.

- Eigen decomposition (EIG)

$$\rho' = \Theta\Lambda\Theta^T \quad (10)$$

where  $\Lambda$  is a diagonal matrix with eigenvalues of the matrix  $\rho'$  and  $\Theta$  is the matrix containing associated eigenvectors.

- Modified Cholesky decomposition (MCHOL)

The MCHOL algorithm is used to avoid numerical problems which are encountered during the comparison. If the matrix  $\rho'$  is a positive-definite matrix, a factorization in Eq. (8) is always found. However, the matrix  $\rho'$  may be negative definite and the factorization is not unique (Higham, 2002). An MCHOL computes a factorization of the positive-definite matrix  $\hat{\rho}' = \rho' + \mathbf{E}$ , where  $\mathbf{E}$  is small. In MCHOL, if a diagonal element is found to be zero, then the entire associated column of  $\mathbf{L}$  is set to zero.

## 3. A simplified analytical model of electric cabinet

### 3.1. Description of the structure and modelling assumptions

The cabinet installed in the laboratory of the Korea Institute of Machinery and Material (Cho et al., 2011) is selected in this research. The dimensions of the cabinet are 150 cm × 80 cm × 65 cm with a mass of 267 kg as shown in Fig. 3(a). The accelerometers are attached to the panel to investigate the dynamic characteristics of the structure.

The cabinet is mounted on a shaking table by welded connections. More details of the experimental setup are presented in Cho et al. (2011).

The analytical model shown in Fig. 3(b) is used to assess the performance of the cabinet due to seismic loadings. The model consists of nonlinear beam elements arranged vertically with lumped mass along the height of the beam. The nonlinear behaviour of the structure is accounted via Duffing's type restoring force (Fig. 3(c)) (Starossek, 2016) for a stress-strain relationship and effects of axial force. Modeling and simulation of the proposed model are implemented in MATLAB with the set of governing equations described in the next section.

### 3.2. Governing equations

For an Euler beam, the relationship between stress ( $\sigma_x$ ) and strain ( $\epsilon_x$ ) of the element can be expressed as (Cho et al., 2011)

$$\sigma_x = E(\epsilon_x - \gamma\epsilon_x^3) \quad (11)$$

where  $E$  is the elastic modulus and  $\gamma$  is the proportional coefficient of strain.

Consider the nonlinear behaviour using the Duffing's equation, the bending moment  $M_n$  can be calculated from the integral of all elemental moments in the form of

$$M_n = \int_A \sigma_x y dA = E \frac{1}{\rho} \int_A y^2 dA - \gamma E \frac{1}{\rho^3} \int_A y^4 dA \quad (12)$$

In the case of rectangular section ( $b \times h$ ), the above equation is given by

$$M_n = \frac{1}{\rho} EI - \beta \frac{1}{\rho^3} EI \quad (13)$$

where  $\beta = \frac{3}{10}\gamma h^2$  and  $EI$  represents the bending stiffness field of the beam element.

Using the relation,  $\frac{1}{\rho} = \frac{d^2y}{dx^2}$ , the deflection equation of a beam with nonlinear bending stiffness is given as follows

$$\frac{d^2y}{dx^2} = \frac{M_n}{EI - \beta EI \left( \frac{d^2y}{dx^2} \right)^2} \quad (14)$$

Then, the strain energy function stored in a beam is derived as follows

$$U = \frac{1}{2} \int_V \sigma_x \epsilon_x dV = \frac{1}{2} EI \int_0^l \left( \frac{\partial^2 y}{\partial x^2} \right)^2 dx - \frac{1}{2} \beta EI \int_0^l \left( \frac{\partial^2 y}{\partial x^2} \right)^4 dx \quad (15)$$

The governing equation of a beam element, considering the nonlinear restoring force, is expressed as

$$[M]_e \{\ddot{U}\}_e + [K]_e \{U\}_e - \beta [K_N]_e \{U^3\}_e = \{F\}_e \quad (16)$$

where  $\{U\}_e$  and  $\{F\}_e$  are displacement and force vectors of beam element, respectively;  $[M]_e$  and  $[K]_e$  are mass and linear stiffness matrices of beam element;  $[K_N]_e$  is nonlinear stiffness matrix of beam element. The mass and stiffness matrices for each element are expressed as follows (Jabboor, 2011; Moon, 2002):

$$[M]_e = \frac{\rho Al}{420} \begin{bmatrix} 156 & 22l & 54 & -13l \\ 22l & 4l^2 & 13l & -3l^2 \\ 54 & 13l & 156 & -22l \\ -13l & -3l^2 & -22l & 4l^2 \end{bmatrix} \quad (17)$$

$$[K]_e = \frac{EI}{l^3} \begin{bmatrix} 12 & 6l & -12 & 6l \\ 6l & 4l^2 & -6l & 2l^2 \\ -12 & -6l & 12 & -6l \\ -6l & 2l^2 & -6l & 4l^2 \end{bmatrix} [K_N]_e \\ = \frac{2EI}{5l^7} \begin{bmatrix} 1296 & 732l^3 & -1296 & 1572l^3 \\ 648l & 176l^4 & -64l & 76l^4 \\ -1296 & -252l & 1296 & -1572l^3 \\ 648l & 76l^4 & -648l & 176l^2 \end{bmatrix} \quad (18)$$

By assembling element matrices, the nonlinear equation of motion (EoM) of the system can be given as follows

$$[M]\{\ddot{U}\} + [K]\{U\} - \beta [K_N]\{U^3\} = \{F\} \quad (19)$$

where  $\{U\}$  and  $\{F\}$  are displacement and force vectors, respectively;  $[M]$  and  $[K]$  are mass and linear stiffness matrices;  $[K_N]$  is nonlinear stiffness matrix.

When axial forces in the beam are considered, stiffness coefficients will be changed. Thus, the EoM in Eq. (19) can be rewritten as

$$[M]\{\ddot{U}\} + [K_C]\{U\} - \beta [K_N]\{U^3\} = \{F\} \quad (20)$$

where  $[K_C] = [K] - [K_G]$  is combined stiffness matrix; and  $[K_G]$  is the global geometric stiffness matrix of the beam and it is defined as (Jabboor, 2011)

$$[K_G]_e = \frac{N}{30l} \begin{bmatrix} 36 & 3l & -36 & 3l \\ 3l & 4l^2 & -3l & -l^2 \\ -36 & -3l & 36 & -3l \\ 3l & -l^2 & -3l & 4l^2 \end{bmatrix} \quad (21)$$

The modal coordinate system can be obtained by using the modal matrix,  $[\Phi]$ , of the system. The displacement,  $\{U\}$ , in the physical coordinate system, can be transformed into the corresponding displacement,  $\{\xi\}$ , in the model coordinate system as follows

$$\{U\} = [\Phi]\{\xi\} \quad (22)$$

Then, the EoM in Eq. (20) can be expressed in the diagonal matrix as

$$\{\ddot{\xi}\} + [\omega_{C,i}^2]\{\xi\} - \beta \left[ \sqrt{\frac{\kappa_{N,i}}{\mu_{C,i}}} \right] \{\xi^3\} = \left[ \sqrt{\frac{1}{\mu_{C,i}}} \right] [\Phi]^T \{F\} \quad (23)$$

In which  $\omega_{C,i}^2 = \frac{\kappa_{C,i}}{\mu_{C,i}}$ .

## 4. Simulation for uncertainties of structural system

### 4.1. Random variations of structural parameters

To consider the variability in the cabinet structure, structural properties are assumed as input random variables. In this research, the stochastic analysis is performed with two parameters such as the modulus of elasticity ( $E$ ) and moment of inertia ( $I$ ). The parameters of these variables are listed in Table 1. The mean values for  $E$  and  $I$  are 210 GPa and  $3.79 \times 10^{-6}$  mm<sup>4</sup>, respectively. The standard deviations and probability distributions are taken based on previous literature (Nowak and Collins, 2012; Waarts and Vrouwenvelder, 1999). The other properties of the cabinet (i.e. height, mass density) are kept constants.

### 4.2. Stochastic motion equations

In this section, a solution for the stochastic analysis with randomization of geometrical and material parameters is given. The solution is developed based on previous discussions. According to this, the stiffness matrices are replaced by functions of random variables. The method is analyzed under various cases to demonstrate the influence of structural properties on the nonlinear response of cabinet structure.

For an element with a variation of elastic modulus and moment of inertia of cross-sections, the bending stiffness,  $(EI)_e(z, x)$ , is a function of these variables (Fig. 4) and it can be expressed as

$$(EI)_e(z, x) = (EI)_e(1 + f_e(z, x)) \quad (24)$$

**Table 1**  
Statistical details of random variables.

Property	Unit	Probability Distribution	Mean	Std.
Modulus of elastic( $E$ )	GPa	Lognormal	210	0.20
Moment of inertia( $I$ )	mm <sup>4</sup>	Normal	$3.79 \times 10^{-6}$	0.15

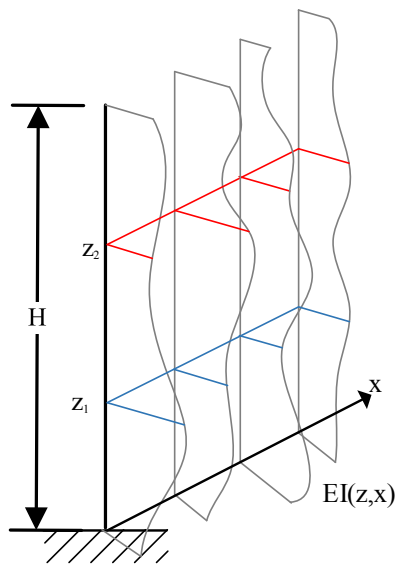


Fig. 4. Ensemble of one-dimensional random field.

where  $(EI)_e$  is the mean value of the bending moment for beam element;  $f_e(z, x)$  is a one-dimensional random field corresponding to the uncertainty of the bending moment. Therefore, the stiffness matrices  $[K]_e$  and  $[K_N]_e$  in Eq. (18) are assumed to be variable  $[\hat{K}]_e$  and  $[\hat{K}_N]_e$  with the parameter  $(EI)_e(z, x)$  and expressed as

$$[\hat{K}]_e = [K]_e(1 + f(z, x)) \quad (25)$$

$$[\hat{K}_N]_e = [K_N]_e(1 + f(z, x)) \quad (26)$$

The displacement in Eq. (22) can be rewritten as follows

$$\{\hat{U}\} = [\hat{\Phi}]\{\hat{\xi}\} \quad (27)$$

With the above description of the process of the random system properties, the Eq. (23) can be rewritten as

$$\ddot{\{\hat{\xi}\}} + [\hat{\omega}_{C,i}^2]\{\hat{\xi}\} - \beta \left[ \sqrt{\frac{\hat{K}_{N,i}}{\mu_{C,i}}} \right] \{\hat{\xi}\}^3 = \left[ \sqrt{\frac{1}{\mu_{C,i}}} \right] [\hat{\Phi}]^T \{F\} \quad (28)$$

## 5. Verification and validation

The numerical model for the cabinet developed in the previous section is first compared to the experimental test for verification purpose. The equation for the nonlinear system in Eq. (23) is solved by using the ODE23 solver in MATLAB, where the input is the acceleration response in time domain obtained in accordance with excitation amplitudes in root mean square (RMS) of 5.8 m/sec<sup>2</sup> (Fig. 5). The proposed model is calibrated and verified with the experimental test via the acceleration response at top of the cabinet.

Fig. 6 shows a comparison of the experimental and numerical models of the acceleration response at the cabinet top. The transfer functions (TF) determined by responses at the top and bottom of the model are performed to obtain fundamental frequencies. The comparison is conducted for dominant frequencies in Fig. 6(b). It can be seen that the TF obtained from the analytical model shifts rightward compared to the experimental test with a difference of 13%. It leads to conclude that the results given by the proposed model are in agreement with experimental results.

## 6. Stochastic structural analysis

In order to evaluate the influences of uncertain material and geometrical properties on dynamic responses of a cabinet, stochastic

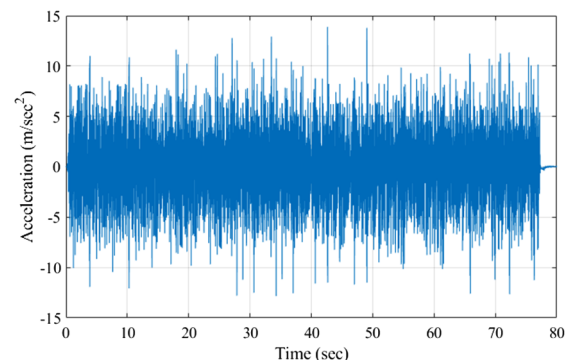


Fig. 5. Acceleration response in the time domain at bottom of the cabinet.

structural analysis is conducted via the schematic diagram in Fig. 1. Based on the above procedure, a MATLAB program has been written for the nonlinear dynamic analysis of the beam stick model with uncertainties of input parameters. The random variables representing the structural properties of the simplified model are described in Section 4. Fig. 4 describes the problem investigated in this research: the spatial variability of structural properties is modelled using random field theory, while the seismic excitation defined at the base of the structure is not taken as input variables. The input ground motion for performing the time history analysis is the Imperial Valley (USA) earthquake of October 15, 1979. The data is recorded by the accelerometer of the Pacific Earthquake Engineering Research Center (PEER) Ground Motion Database with the peak ground motion (PGA) and time interval are 0.315 g and 0.01 s, respectively. Details of time history and resulting response spectrum are shown in Fig. 7.

The output responses are carried out by stochastic analysis of nine cases, which are: three decomposition methods (i.e. CHOL, EIG, and MCHOL) for three input variable cases (i.e. elastic modulus ( $E$ ), moment of inertia ( $I$ ), and both elastic modulus and moment of inertia ( $EI$ )). The effectiveness of each case is compared with the result observed by the deterministic analysis (DA). The DA is performed with the case where no variation is applied in the structural properties.

### 6.1. Free vibration response of the cabinet

Dynamic characteristics of the electrical cabinet are essential response parameters for its dynamic behaviour. Stochastic natural frequencies of the cabinet with randomization of input variables are calculated for different decomposition methods. A comparison between the statistical distributions of the first fundamental frequencies obtained from all cases is illustrated in Fig. 8 and summarized in Table 2. The first natural frequency from DA (15.12 Hz) is used as a reference solution for comparison purpose.

The first column in Fig. 8 reports probabilistic distributions of frequencies obtained from uncertain elastic modulus using various methods. It can be seen that the mean natural frequency of MCHOL method is in close agreement with the deterministic result (error = 0.726%) while error values are 0.968% and 1.024% in the case of CHOL and EIGEN, respectively. Moreover, the highest standard deviation produced by CHOL method (1.425 Hz) indicates more dispersion of the response. Based on the observed results, it can be concluded that the performance of MCHOL is better than other methods.

Stochastic natural frequencies by various input variables of  $E$ ,  $I$  and  $EI$  using the CHOL method are compared in the first row of Fig. 8. It is inferred that the dispersions of output fundamental frequencies increase with the increment of the number of input random variables. This observation can be explained from standard deviations in Table 2. When allowing simultaneous uncertainty in  $EI$ , the histogram shows the largest dispersion in the probabilistic distribution of frequency with

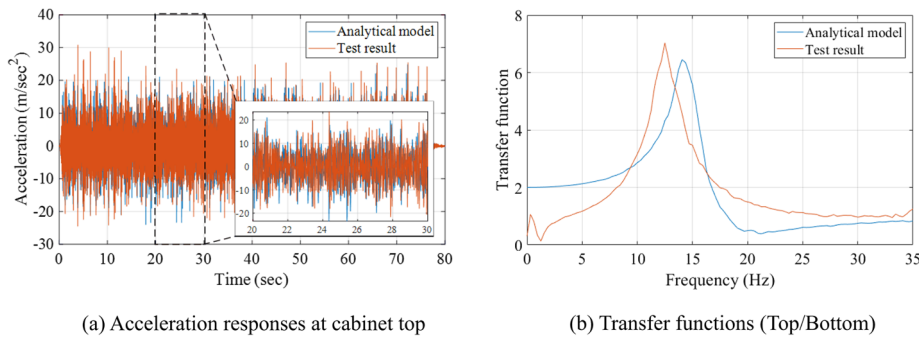


Fig. 6. Comparison of acceleration responses between experimental test and analytical model.

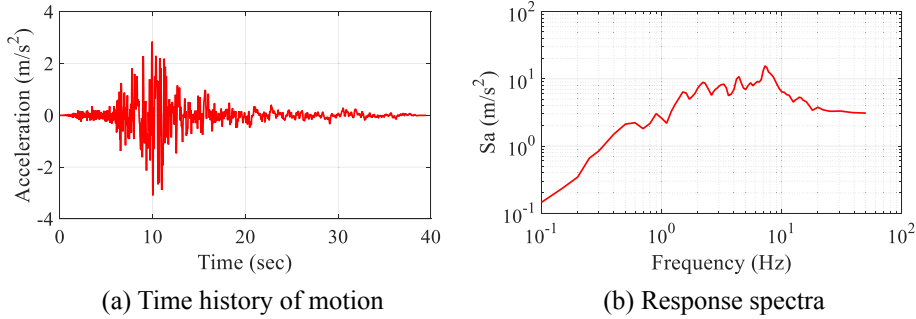


Fig. 7. Accelerometer record of the Imperial Valley earthquake.

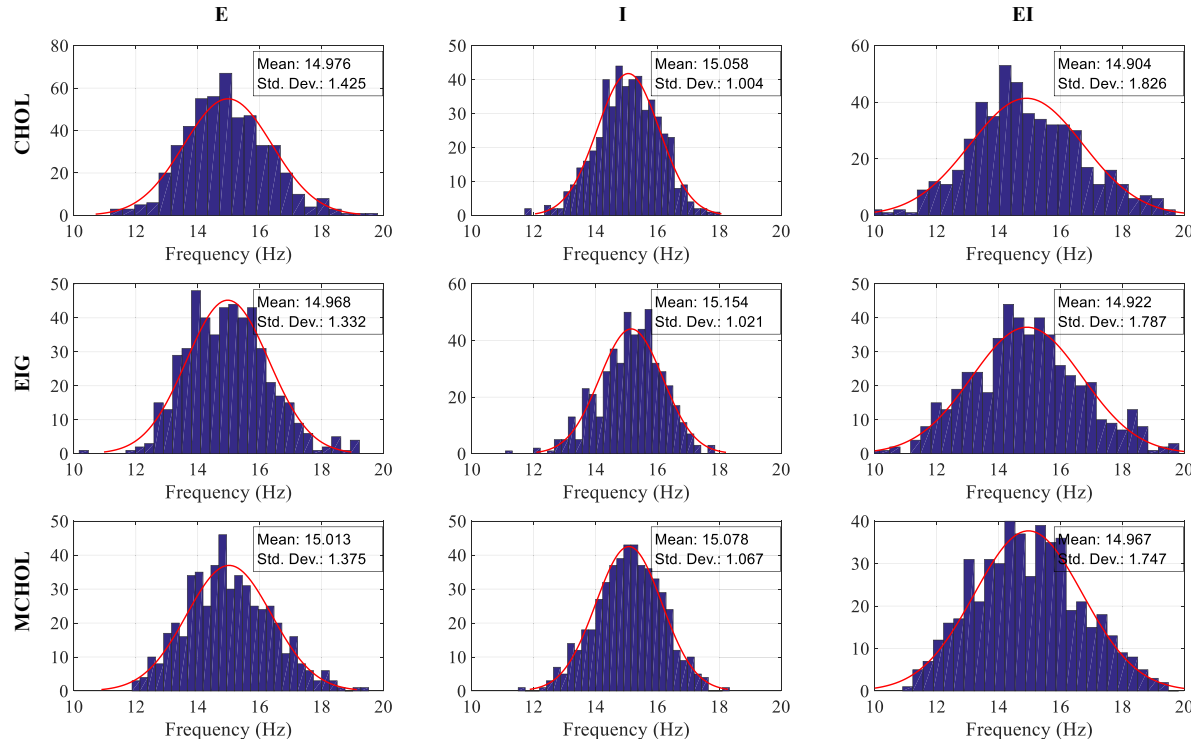


Fig. 8. Probabilistic distributions of first natural frequencies.

**Table 2**

Statistical parameters of first natural frequency obtained from different cases.

Parameters	Methods	Max (Hz)	Min (Hz)	Mean (Hz)	Std. Dev. (Hz)	Error (%)
E	CHOL	22.952	11.176	14.976	1.425	0.968
	EIGEN	19.227	10.168	14.968	1.332	1.024
	MCHOL	19.523	11.876	15.013	1.375	0.726
I	CHOL	18.023	11.714	15.058	1.004	0.428
	EIGEN	17.856	11.088	15.154	1.021	0.207
	MCHOL	18.328	11.502	15.078	1.067	0.295
EI	CHOL	20.848	9.479	14.904	1.826	1.446
	EIGEN	19.829	9.820	14.922	1.787	1.327
	MCHOL	20.811	10.901	14.967	1.747	1.029

a maximum value of standard deviation (1.826 Hz). This indicates the importance of the random input variables when the cabinet structure is subjected to earthquake loadings.

In addition, statistical analyses computed for each random variable are also presented in [Table 2](#). The results show that the natural frequencies exhibit variations as a function of input random fields and decomposition methods. When assuming the spatial variability in a moment of inertia, the result gives less error in structural dynamic characteristic. This implies that the geometrical property imparted to the cabinet structure is less effective in stochastic structural analysis. In contrast, the natural frequency shows a higher error when the uncertain elastic modulus is considered, which implies that the material property imparted to the cabinet structure accounts for an important proportion of the cabinet stiffness.

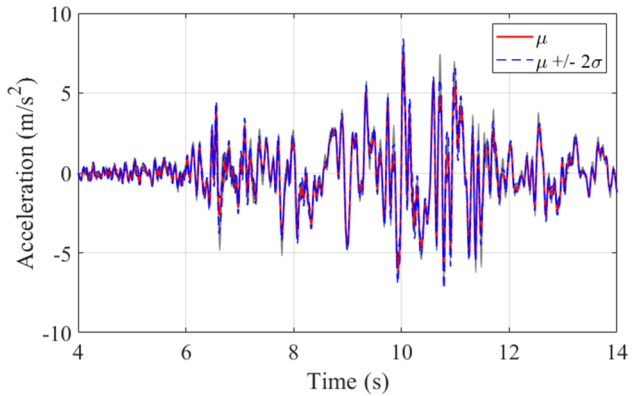
## 6.2. Nonlinear response of the cabinet

The nonlinear response of cabinet due to uncertainty in structural properties is presented herein. The different decomposition methods in the CMD generator are used to obtain stochastic responses of the structure. The effectiveness of each method for various input variables is studied for displacement and acceleration responses at the top of the cabinet.

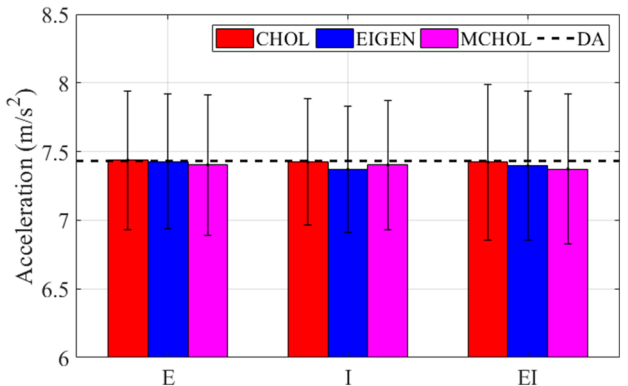
### 6.2.1. Effects on acceleration responses

[Fig. 9](#) and [Table 3](#) demonstrate acceleration responses at the cabinet top carried out by stochastic analysis for all cases. As shown in [Fig. 9\(a\)](#), the acceleration response due to the randomization of elastic modulus using the CHOL decomposition is displayed. Results are presented in the form of all simulations, mean ( $\mu$ ), and the mean  $\pm 2 \times$  standard deviation ( $\mu \pm 2\sigma$ ). The  $\mu$  and  $\sigma$  values for all cases are plotted in [Fig. 9\(b\)](#). These results are compared with the reference solution that is represented by a horizontal dash line. In general, the mean responses for all cases are in good agreement with the result of DA. For CHOL method, the dispersion in case of a moment of inertia is  $0.459 \text{ m/s}^2$  while the result in case of elastic modulus is  $0.504 \text{ m/s}^2$ . The largest dispersion is given for uncertainty in EI with a value of  $0.568 \text{ m/s}^2$ . For MCHOL method, the dispersions obtained from the random field E, I, and EI are 0.511, 0.469, and  $0.547 \text{ m/s}^2$ , respectively. More detailed data are summarized in [Table 3](#). Furthermore, the differences between the dispersions of accelerations are depicted in [Fig. 9\(c\)](#). The distribution of responses is assumed to follow the normal distribution. Although the dispersion of all three input variables is similar, the randomization of EI has a slight higher dispersion. Based on the obtained results, the dispersion in output responses increases whenever there is the increment of a number of input random variables.

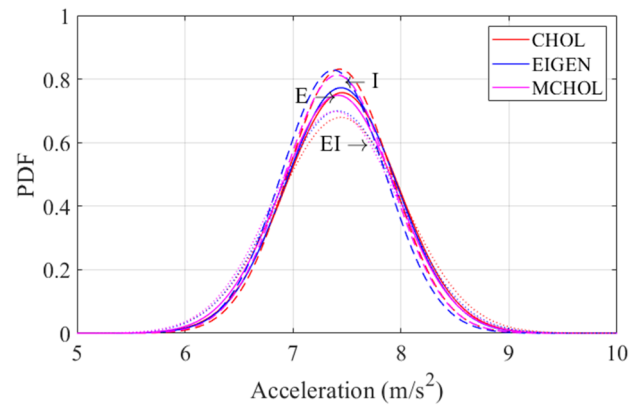
The discrepancies in acceleration at the top of the cabinet obtained



(a) Acceleration responses at cabinet top



(b) Mean and standard deviation of the acceleration responses

(c) Acceleration dispersion  
(Solid = E, Dashed = I, Dotted = EI)

[Fig. 9](#). Summary of acceleration response results for all cases.

from different models are also explained through cumulative distribution function (CDF). The CDF of a probability distribution is a function that defines the probability of the random variable which takes a value less than or equal to  $x$  and is expressed as:

$$F(x) = P(X \leq x) \quad (29)$$

The sensitivity of acceleration responses for the various models is

**Table 3**  
Statistical parameters of accelerations obtained from different cases.

Parameters	Methods	Max (m/s <sup>2</sup> )	Min (m/s <sup>2</sup> )	Mean (m/s <sup>2</sup> )	Std. (m/s <sup>2</sup> )	Error (%)
E	CHOL	8.352	6.190	7.437	0.504	0.071
	EIG	8.153	6.502	7.427	0.491	0.064
	MCHOL	8.046	6.503	7.403	0.511	0.387
I	CHOL	8.168	6.503	7.424	0.459	0.101
	EIG	8.354	6.504	7.369	0.461	0.836
	MCHOL	8.284	6.503	7.401	0.469	0.402
EI	CHOL	9.592	6.345	7.423	0.568	0.115
	EIG	8.404	6.502	7.396	0.544	0.478
	MCHOL	8.324	6.350	7.373	0.547	0.789

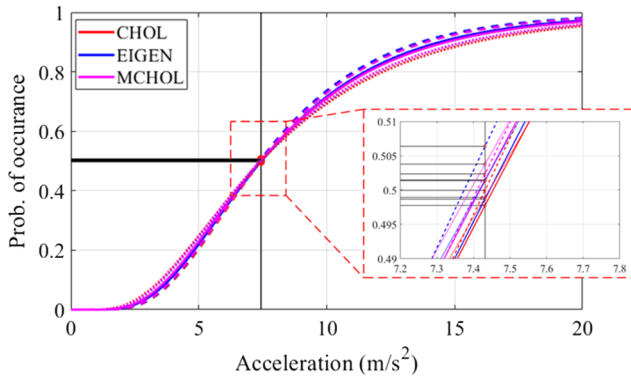
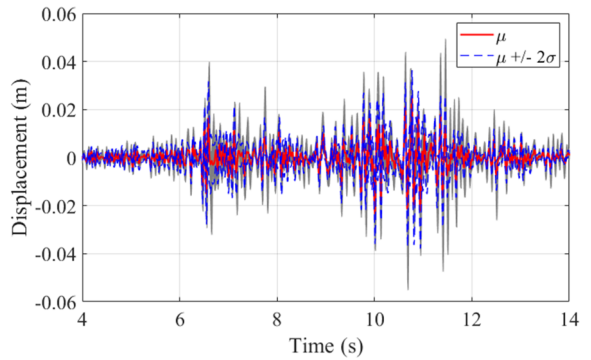


**Fig. 10.** Cumulative distribution functions of accelerations for various models (Solid = E, Dashed = I, Dotted = EI).

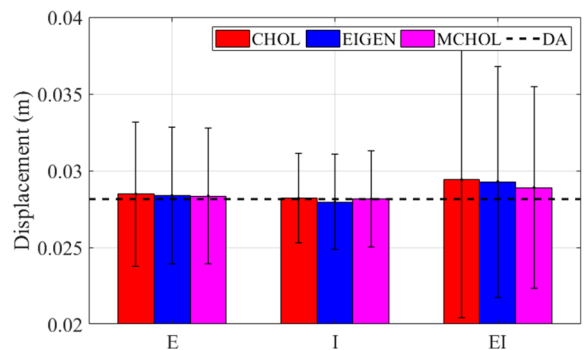
evaluated through CDF graph in Fig. 10. The response from DA ( $7.431 \text{ m/s}^2$ ) is used to consider the change in the cumulative distribution function of acceleration with other cases. The change in the probability of acceleration for different cases is summarized in Table 4. This table shows that the moment of inertia gives the highest probabilities of acceleration response with the corresponding values for CHOL, EIG, and MCHOL are 50%, 50.64%, and 50.24%, respectively.

#### 6.2.2. Effects on displacement responses

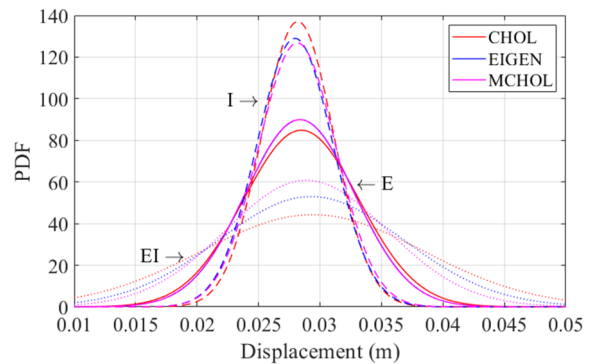
The influence of all input variables on the displacement responses at the top of the cabinet is displayed in Fig. 11. Similar to the previous section, Fig. 11(a) describes the displacement response that allows the randomization of elastic modulus using the CHOL decomposition. The statistical parameters of output responses for all cases are plotted in Fig. 11(b)–(c) and tabulated in Table 5. As shown in Fig. 11(b), two data series are displayed corresponding to the deterministic (horizontal dash line) and random variables (column). The results show that responses in random variables tend to overestimate the response compared to DA ( $2.814 \text{ cm}$ ), except in the case of using the EIG decomposition method for the uncertain moment of inertia (error = 0.652%). In order to evaluate the dispersions of displacement responses of the cabinet, the mean and standard deviation for all cases are shown in Fig. 11(c). For all decomposition methods, the displacement responses in case of randomness moment of inertia,  $I$ , exhibit smaller dispersion than those of other input variables ( $E$  and  $EI$ ). Among the



(a) Displacement responses at cabinet top



(b) Mean and standard deviation of the displacement responses



(c) Displacement dispersion  
(Solid = E, Dashed = I, Dotted = EI)

**Fig. 11.** Summary of displacement response results for all cases.

decomposition methods, MCHOL produces the lowest dispersion. The values of standard deviations are  $0.444 \text{ cm}$ ,  $0.315 \text{ cm}$ , and  $0.656 \text{ cm}$  for  $E$ ,  $I$  and  $EI$ , respectively.

Additionally, the errors of the responses compared to the DA are shown in the last column of Table 5. Three data series are provided, corresponding to the material property, geometrical property, and the

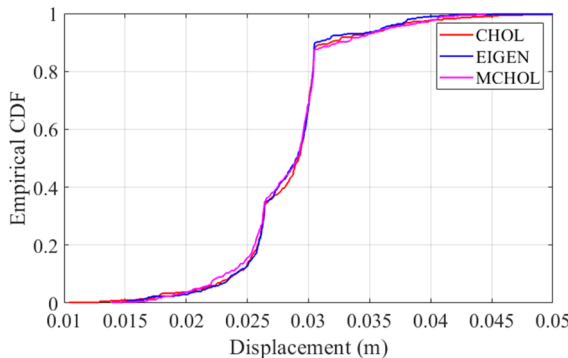
**Table 4**  
Changes in the probability of acceleration from different cases.

	E			I			EI		
	CHOL	EIGEN	MCHOL	CHOL	EIGEN	MCHOL	CHOL	EIGEN	MCHOL
Value of probability (%)	49.78	49.87	50.14	50	50.64	50.24	49.89	50.15	50.38

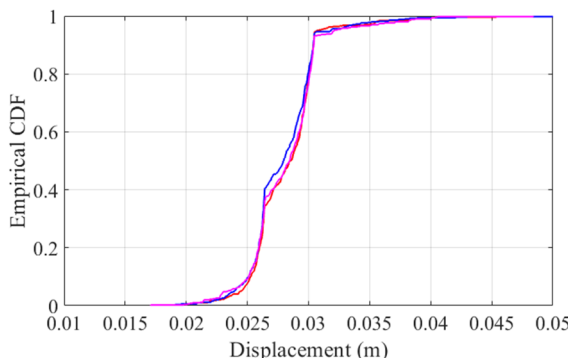
**Table 5**

Statistical parameters of displacements obtained from different cases.

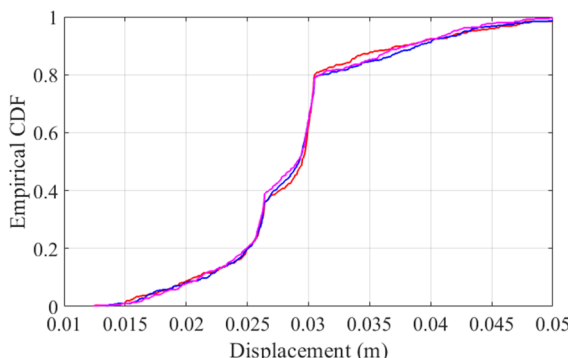
Parameters	Methods	Max (cm)	Min (cm)	Mean (cm)	Std. (cm)	Error (%)
E	CHOL	5.519	1.039	2.848	0.470	1.189
	EIG	7.028	1.458	2.837	0.443	0.807
	MCHOL	4.453	1.391	2.835	0.444	0.741
I	CHOL	4.604	1.822	2.819	0.291	0.169
	EIG	5.704	1.884	2.796	0.309	0.652
	MCHOL	4.839	1.709	2.815	0.315	0.015
EI	CHOL	11.180	1.241	2.940	0.901	4.472
	EIG	8.492	1.346	2.928	0.753	4.055
	MCHOL	6.038	1.244	2.890	0.656	2.677



(a) Elastic modulus



(b) Moment of inertia



(c) Elastic modulus and Moment of inertia

**Fig. 12.** Empirical response CDF.

combination of material and geometrical properties. In all cases, the MCHOL shows a good match between the DA and random field results. For three input variable cases, the randomness in *EI* shows a larger error in term of response. This demonstrates that as a number of random field increases, the response of the cabinet increases as well. In order to quantify the uncertainty in the displacement response due to the randomness of input variables, the empirical cumulative distribution functions (CDF) for the output responses are illustrated in Fig. 12. Details of histograms and the empirical CDF of input random variables using decomposition methods on the displacement responses are discussed in Fig. 13.

## 7. Conclusions

Uncertainty quantification in structural seismic responses is critical for cabinet facility while most of the current studies are limited to homogeneous input variables. This research is to focus on the randomness in structural properties of the electric cabinet. The influences of the random variables are examined via random field theory. The random field generator is applied based on the covariance matrix decomposition (i.e. Cholesky, Eigen, and modified Cholesky decompositions) and a midpoint discretization method. The following are the main contributions of the present study.

- A solution of nonlinear stochastic equations of motions for the beam stick model of cabinet structures is presented.
- The random field theory is proposed for considering the uncertainty in geometrical and material properties of the cabinet.
- The effects of decomposition methods on structural responses are evaluated.
- In order to consider the impact of nonlinear behaviour on the cabinet, the different outputs are studied.
- Finally, the probabilistic evaluation is conducted for the cabinet facility due to seismic loadings.
- The effects of input parameters on the distributions of the free vibration, acceleration, and displacement responses are also observed. The following findings are drawn:
- A simplified model considering the effects of axial force and Duffing's type restoring force has been developed for the cabinet in nuclear power plants. The adaptability of the analytical model is verified based on the agreement on responses with the experiment. It was found that the transfer function produced by the proposed model shifts rightward compared to the experimental result with an increase of 13%.
- The results of the heterogeneity in structural properties confirm that the uncertain geometrical property has a low effect on the seismic

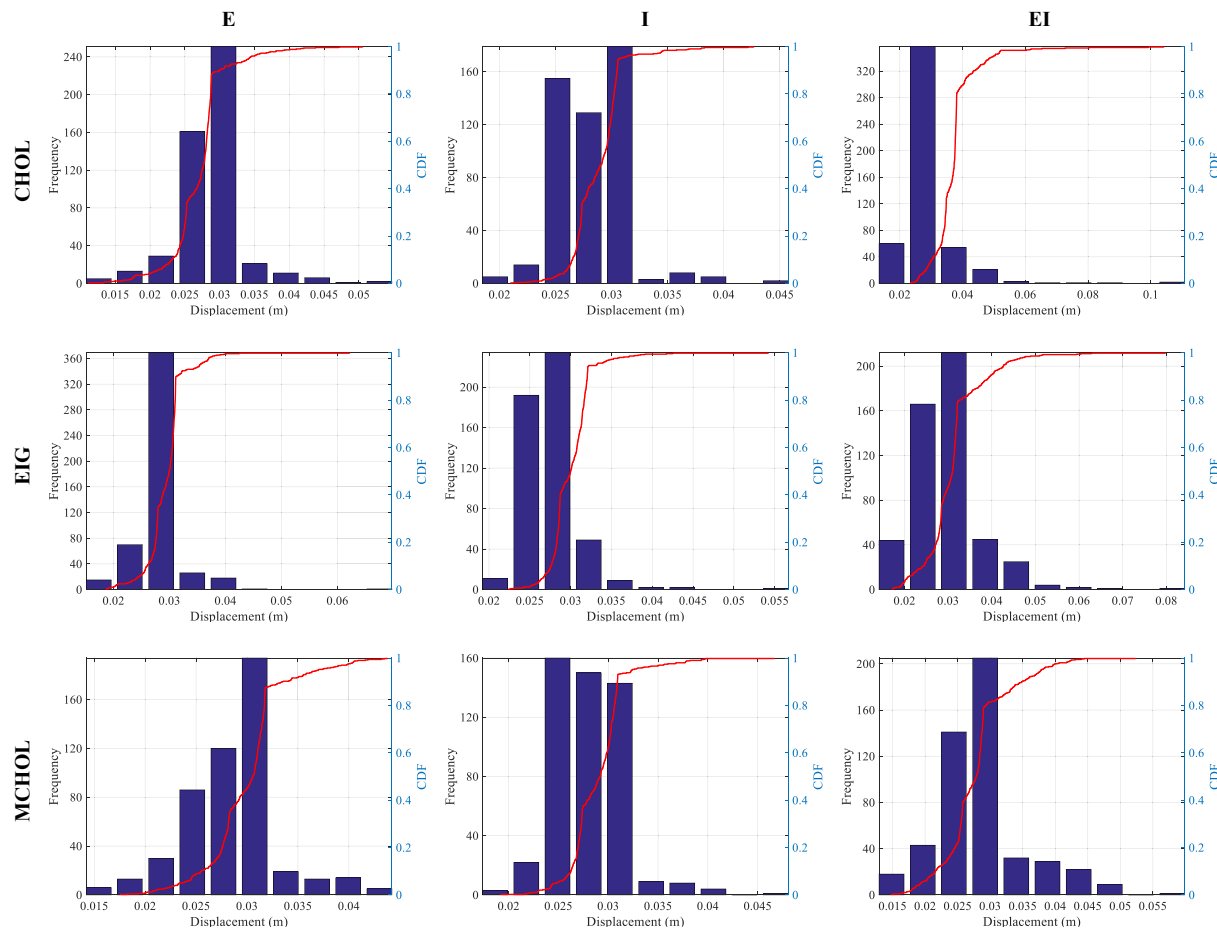


**Fig. 13.** Detailed empirical CDF of displacement responses.

vulnerability assessment of cabinet facility. The probabilistic distributions for this variable show the lowest error of natural frequencies with values of 0.428%, 0.207% and 0.295% for CHOL, EIG, and MCHOL decompositions, respectively.

- The response dispersions (i.e. displacement and acceleration) depend on the contribution of a number of input variables. When allowing simultaneous uncertainty in elastic modulus and moment of inertia (*EI*), the dispersion is the highest compared to the case with only one random variable (i.e. *E* and *I*).
- It is indicated that the MCHOL method is in close agreement with the deterministic result. The randomness in material property produces error values of 0.968%, 1.024% and 0.726% for CHOL, EIG, and MCHOL decompositions, respectively. When assuming two random variables, the errors have a slight higher compared to the other cases.

## Acknowledgments

This work was supported by the Korea Institute of Energy Technology Evaluation and Planning (KETEP) and the Ministry of Trade, Industry & Energy (MOTIE) of the Republic of Korea (No. 20171510101960).

## Appendix A. Supplementary data

Supplementary data to this article can be found online at <https://doi.org/10.1016/j.nucengdes.2019.110309>.

## References

- Cho, S.G., Kim, D., Chaudhary, S., 2011. A simplified model for nonlinear seismic response analysis of equipment cabinets in nuclear power plants. *Nucl. Eng. Des.* 241 (8), 2750–2757.
- Eem, S., Kim, J.H., 2019. Sensitivity analysis for the distribution of maximum responses by seismic isolation system parameters using the stochastic response database. *Nucl. Eng. Des.* 347, 53–58.
- Griffiths, D.V., Huang, J., Fenton, G.A., 2009. Influence of spatial variability on slope reliability using 2-D random fields. *J. Geotech. Geo-environ. Eng.* 135 (10), 1367–1378.
- Gupta, A., Rustogi, S.K., Gupta, A.K., 1999. Ritz vector approach for evaluating incabinet response spectra. *Nucl. Eng. Des.* 190 (3), 255–272.
- Gupta, A., Yang, J., 2002. Modified Ritz vector approach for dynamic properties of electrical cabinets and control panels. *Nucl. Eng. Des.* 217 (1–2), 49–62.
- Higham, N.J., 2002. Accuracy and Stability of Numerical Algorithms, vol. 80. Siam, Philadelphia, PA.
- Hur, J., 2012. Seismic Performance Evaluation of Switchboard Cabinets Using Nonlinear Numerical Models. Doctoral dissertation. Institute of Technology, Georgia.
- Jabboor, W., 2011. Dynamic Structural Analysis of Beams. Doctoral dissertation. Heriot-Watt University.
- Jenkel, C., Leichsenring, F., Graf, W., Kaliske, M., 2015. Stochastic modelling of uncertainty in timber engineering. *Eng. Struct.* 99, 296–310.
- Kala, Z., 2011. Sensitivity analysis of stability problems of steel plane frames. *Thin-Walled Struct.* 49 (5), 645–651.
- Kim, M.K., Choi, I.K., Seo, J.M., 2012. A shaking table test for an evaluation of seismic behavior of 480 V MCC. *Nucl. Eng. Des.* 243, 341–355.
- Koo, K.Y., Cho, S.G., Cui, J., Kim, D., 2010. Seismic response prediction for cabinets of nuclear power plants by using impact hammer test. *Nucl. Eng. Des.* 240 (10), 2500–2511.
- Kotelko, M., Lis, P., Macdonald, M., 2017. Load capacity probabilistic sensitivity analysis of thin-walled beams. *Thin-Walled Struct.* 115, 142–153.
- Lim, E., 2016. A Method for Generating Simplified Finite Element Models for Electrical Cabinets. Doctoral dissertation. Institute of Technology, Georgia.
- Moon, B., 2002. Study of Vibration Analysis of Nonlinear Rotor System Using Analytical Method. Doctoral dissertation. Department of Mechanical Design Engineering, Kobe University, Kobe, Japan.
- Nguyen, P.C., Kim, S.E., 2014. Nonlinear inelastic time-history analysis of three-

- dimensional semi-rigid steel frames. *J. Constr. Steel Res.* 101, 192–206.
- Nguyen, D.D., Thusa, B., Han, T.S., Lee, T.H., 2019. Identifying significant earthquake intensity measures for evaluating seismic damage and fragility of nuclear power plant structures. *Nucl. Eng. Technol.*
- Nowak, A.S., Collins, K.R., 2012. Reliability of Structures. CRC Press, Boca Raton, FL.
- Bandyopadhyay, K.K., Hofmayer, C.H., Kassir, M.K., Pepper, S.E., 1987. Seismic Fragility of Nuclear power plant Components: Phase 2, Motor Control Center, Switchboard, Panelboard and Power Supply. No. NUREG/CR-4659-VOL. 2. Brookhaven National Lab.
- Sahu, D., Nishanth, M., Dhir, P.K., Sarkar, P., Davis, R., Mangalathu, S., 2019. Stochastic response of reinforced concrete buildings using high dimensional model representation. *Eng. Struct.* 179, 412–422.
- Starossek, U., 2016. Exact analytical solutions for forced undamped Duffing oscillator. *Int. J. Non Linear Mech.* 85, 197–206.
- Thai, D.K., Kim, S.E., 2015. Safety assessment of a nuclear power plant building subjected to an aircraft crash. *Nucl. Eng. Des.* 293, 38–52.
- Tran, T.T., Nguyen, T.H., Kim, D., 2018a. Seismic incidence on base-isolated nuclear power plants considering uni-and bi-directional ground motions. *J. Struct. Integrity Maint.* 3 (2), 86–94.
- Tran, T.T., Han, S.R., Kim, D., 2018b. Effect of probabilistic variation in soil properties and profile of site response. *Soils Found.* 58 (6), 1339–1349.
- Tran, T.T., Cao, A.T., Nguyen, T.H.X., Kim, D., 2019. Fragility assessment for electric cabinet in nuclear power plant using response surface methodology. *Nucl. Eng. Technol.* 51 (3), 894–903.
- Vanmarcke, E., 1982. Developments in random field modelling. *Nucl. Eng. Des.* 71 (3), 325–327. [https://doi.org/10.1016/0029-5493\(82\)90100-5](https://doi.org/10.1016/0029-5493(82)90100-5).
- Vanmarcke, E., 2010. Random Fields: Analysis and Synthesis. World Scientific.
- Van der Have, R.C., 2015. Random Fields for Non-linear Finite Element Analysis of Reinforced Concrete. Master's dissertation. Delft University of Technology, the Netherlands.
- Waarts, P.H., Vrouwenvelder, A.C.W.M., 1999. Stochastic finite element analysis of steel structures. *J. Constr. Steel Res.* 52 (1), 21–32.
- Wang, Z., Pedroni, N., Zentner, I., Zio, E., 2018. Seismic fragility analysis with artificial neural networks: application to nuclear power plant equipment. *Eng. Struct.* 162, 213–225.
- Xu, X.F., 2011. Reliability-based Design in Geotechnical Engineering: Computations and Applications. CRC Press, Boca Raton, FL.
- Yue, Q., Ang, A.H.S., 2017. 3D reliability evaluation of tunnels under strong-motion earthquakes considering spatial randomness. *Struct. Infrastruct. Eng.* 13 (7), 882–893.